Proc. 6th Asian Conference on Computer Vision (ACCV 2004), January 2004, Jeju, Korea, Vol. 2, pp. 1128–1133.

ROBUST IMAGE MATCHING PRESERVING GLOBAL CONSISTENCY

Yasushi Kanazawa[*] *and Kenichi Kanatani*[†]

[*]Department of Knowledge-based Information Engineering
Toyohashi University of Technology, Toyohashi, Aichi 441-8580 Japan
[†]Department of Information Technology, Okayama University, Okayama 700-8530 Japan
kanazawa@tutkie.tut.ac.jp, kanatani@suri.it.okayama-u.ac.jp

ABSTRACT

We present a new method for detecting point matches between two images. While existing methods propagate local smoothness by iterations, our method imposes non-local constraints that should be approximately satisfied across the image. We define the "confidence" of such "soft constraints" to all potential matches. The confidence is progressively updated by "mean-field approximation". Finally, the "hard" epipolar constraint is imposed by RANSAC. Using real images, we demonstrate that our method is robust to camera rotations and zooming changes.

1. INTRODUCTION

Establishing point correspondences over multiple images is the first step of many computer vision applications. Two approaches exist for this purpose: tracking correspondences over successive frames, and direct matching between separate frames. This paper focuses on the latter.

The basic principle is local correlation measurement. Extracting feature points in the first and second images separately using a corner detector [3, 5, 17, 19, 20, 21], we measure the correlation between the neighborhoods of the two points for each candidate pair and match those that have a high correlation. This works very well if one image is a translated copy of the other. For images taken from different positions, however, the corresponding parts in the images may be locally deformed. In particular, the correlation significantly diminishes if camera rotations or zooming changes take place.

It follows that additional constraints are necessary. If the scene is a planar surface or in the distance, the two images are related by a *homography* [6]. This strong constraint can be combined with voting techniques such as LMedS [18] and RANSAC [4] for robust image matching [7, 10, 11].

For a general scene, the only available constraint is the *epipolar equation* [6], and various types of voting schemes based on it have been proposed [1, 6, 22, 23, 25]. However, the epipolar equation is a very weak constraint, admitting many unnatural and inconsistent matches.

To resolve this, some global consistency condition that favors "natural" matches is necessary. A typical approach is to define a local similarity measure and search for a global match that maximizes the total similarity. Since the solution is a permutation matrix with at most 1 in each row and column and 0 elsewhere, this is a very difficult integer programming task.

In order to alleviate this, many approximation schemes have been proposed including replacing the permutation matrix by a real matrix [13, 14, 24], tensor voting [12], combining the distant transform with hierarchical search [15], relaxation of graph labels [25], multiresolution approaches [2], and graph partition algorithms [16]. Still, a large amount of computations is necessary. Also, because local similarity is iteratively propagated, we cannot impose global conditions on spatially apart matches directly.

In this paper, we present an algorithm that does not involve such iterative propagation. Instead, global consistency is imposed on all potential matches directly. We require correct matches to be spatially smooth, assuming that the scene is more or less planar or in the distance.

The main difficulty is how to deal with requirements that should be satisfied "approximately". For example, if two points have low image correlations, we cannot deny the possibility that they may match. Similarly, non-smooth or seemingly inconsistent matches can be correct. We say such violable constraints are *soft* while inviolable constraints such as the epipolar equation are *hard*.

Our strategy is to define to *all* potential matches *confidence values* that measure the degree of satisfaction of the constraints. Then, we select high confidence matches and estimate from them the global properties, from which the confidence values of all potential matches are updated. This scheme resembles the *mean-field approximation* used in physics. Finally, the hard epipolar constraint is strictly imposed by RANSAC. Using real images, we demonstrate that our method is robust to camera rotations and zooming changes.

2. TEMPLATE MATCHING

We measure the local correlations between points p and q by the *residual* (*sum of squares*)

$$J(p,q) = \sum_{(i,j)\in\mathcal{N}} |T_p(i,j) - T_q(i,j)|^2, \qquad (1)$$

where $T_p(i,j)$ and $T_q(i,j)$ are the intensity values of the templates defined by cutting out an $w \times w$ pixel region $\mathcal{N}$ centered on p and q, respectively[1]. If we normalize them to $\sum_{(i,j)\in\mathcal{N}} T_p(i,j)^2 = 1$ and $\sum_{(i,j)\in\mathcal{N}} T_q(i,j)^2 = 1$, eq. (1) is equivalent to the use of the *normalized correlation*.

We extract N points p_1, ..., p_N in the first image and M points q_1, ..., q_M in the second, using a corner detector. Then, we compute the residuals $\{J(p_\alpha, q_\beta)\}$, $\alpha = 1, ..., N$, $\beta = 1, ..., M$, for all their NM combinations and search the $N \times M$ table of $\{J(p_\alpha, q_\beta)\}$ for the minimum value $J(p_{\alpha^*}, q_{\beta^*})$, establishing the match between points p_{α^*} and q_{β^*}. Then, we remove from the table the column and row that contain the value $J(p_{\alpha^*}, q_{\beta^*})$ and do the same procedure to the resulting $(N-1) \times (N-1)$ table. Repeating this, we end up with $L = \min(N, M)$ matches. We call this *uniqueness enforcement* with respect to the residual J.

However, this procedure cannot be done directly, since the selected pairs may not be all correct while some of the discarded pairs may be correct. In order to take all potential matches into consideration, we introduce confidence values to all pairs.

3. CONFIDENCE OF LOCAL CORRELATIONS

We define the confidence of local correlations for the pair (p, q) via the *Gibbs distribution* in the form

$$P = e^{-sJ(p,q)}, \tag{2}$$

so that high confidence is given for a smaller residual $J(p,q)$. Physicists usually put $s = 1/kT$ and call T *temperature*, where k is the Boltzmann constant. If $s = 0$ (or $T = \infty$), we have uniformly $P = 1$ irrespective of the residual $J(p,q)$. As s increases (or T decreases), the confidence of those with large residuals quickly decreases, and ultimately the confidence concentrates only on the smallest residual.

Here, we determine the attenuation constant s (or temperature T) as follows. Among all the NM pairs $\{(p_\alpha, q_\beta)\}$, at most L (= $\min(N, M)$) can be correct. We require that the average of the L smallest residuals equal the overall weighted average with respect to the confidence (2). If the NM potential matches (p_α, q_β) are sorted in ascending order of $J(p_\alpha, q_\beta)$ and the λth residual is abbreviated as J_λ, this condition is written in the form

$$\frac{1}{Z}\sum_{\lambda=1}^{NM} J_\lambda e^{-sJ_\lambda} = \bar{J}, \tag{3}$$

where

$$Z = \sum_{\lambda=1}^{NM} e^{-sJ_\lambda}, \qquad \bar{J} = \frac{1}{L}\sum_{\lambda=1}^{L} J_\lambda. \tag{4}$$

The solution of eq. (3) is easily computed by Newton iterations to search for the zero of $\Phi(s) = 0$, starting from $s = 0$, where we define

$$\Phi(s) = \sum_{\lambda=1}^{NM} (J_\lambda - \bar{J}) e^{-sJ_\lambda}. \tag{5}$$

Let $P_\lambda^{(0)}$ be the confidence of local correlations for the λth pair thus defined.

4. CONFIDENCE OF SPATIAL CONSISTENCY

Next, we introduce the confidence of spatial consistency, assuming that the scene does not have an extraordinary 3-D shape. We first choose candidate matches by enforcing uniqueness with respect to $P_\lambda^{(0)}$ to those pairs that satisfy[2]

$$P_\lambda^{(0)} > e^{-k^2/2}. \tag{6}$$

We enumerate the resulting matches by the index $\mu = 1$, ..., n_0 in an arbitrary order. Let $\vec{r}_\mu$ be the 2-dimensional vector that connects the two points of the μth match, starting from the one in the first image and ending at the other in the second. We call it the "flow vector" of the μth match.

Our strategy is to view those matches which are consistent with the resulting "optical flow" $\{\vec{r}_\mu\}$ as more likely to be correct. Specifically, we compute the confidence weighted mean $\vec{r}_m$ and the confidence weighted covariance matrix V of the optical flow by

$$\vec{r}_m = \frac{1}{Z}\sum_{\mu=1}^{n_0} P_\mu^{(0)} \vec{r}_\mu, \qquad Z = \sum_{\mu=1}^{n_0} P_\mu^{(0)},$$
$$V = \frac{1}{Z}\sum_{\mu=1}^{n_0} P_\mu^{(0)} (\vec{r}_\mu - \vec{r}_m)(\vec{r}_\mu - \vec{r}_m)^\top. \tag{7}$$

Then, we go back to the original NM potential matches. We define their confidence of spatial consistency via the Gaussian distribution in the form

$$P_\lambda^{(1)} = e^{-(\vec{r}_\lambda - \vec{r}_m, V^{-1}(\vec{r}_\lambda - \vec{r}_m))}, \tag{8}$$

where $(\vec{a}, \vec{b})$ designates the inner product of vectors $\vec{a}$ and $\vec{b}$. Thus, a flow vector $\vec{r}_\lambda$ has low confidence if it largely deviates from the optical flow $\{\vec{r}_\mu\}$.

5. CONFIDENCE OF GLOBAL SMOOTHNESS

We then introduce the confidence of global smoothness, assuming that the scene is more or less planar or in the distance so that the image transformation can be roughly approximated by a homography.

First, we choose candidate matches. This time, we enforce uniqueness with respect to $P_\lambda^{(0)} P_\lambda^{(1)}$ to those pairs that satisfy

$$P_\lambda^{(0)} P_\lambda^{(1)} > e^{-2k^2/2}. \tag{9}$$

[1] We let $w = 9$ in our experiments.

[2] we let $k = 3$ in our experiment.

We enumerate the resulting matches by the index μ = 1, ..., n_1 in an arbitrary order.

Let (x_μ, y_μ) and (x'_μ, y'_μ) make the μth pair. We represent these two points by 3-D vectors

$$\boldsymbol{x}_\mu = \begin{pmatrix} x_\mu/f_0 \\ y_\mu/f_0 \\ 1 \end{pmatrix}, \quad \boldsymbol{x}'_\mu = \begin{pmatrix} x'_\mu/f_0 \\ y'_\mu/f_0 \\ 1 \end{pmatrix}, \tag{10}$$

where f_0 is an appropriate scale factor, e.g., the image size. A homography is written in the form

$$\boldsymbol{x}' = Z[\boldsymbol{H}\boldsymbol{x}], \tag{11}$$

where $Z[\,\cdot\,]$ means normalization to make the third component 1. We optimally fit a homography to the n_1 candidate matches. Let the true positions of $\{\boldsymbol{x}_\mu\}$ and $\{\boldsymbol{x}'_\mu\}$ be, respectively, $\{\bar{\boldsymbol{x}}_\mu\}$ and $\{\bar{\boldsymbol{x}}'_\mu\}$. Taking account of their confidence, we minimize

$$J = \sum_{\mu=1}^{n_1} P_\mu^{(0)} P_\mu^{(1)} (\|\boldsymbol{x}_\mu - \bar{\boldsymbol{x}}_\mu\|^2 + \|\boldsymbol{x}'_\mu - \bar{\boldsymbol{x}}'_\mu\|^2), \tag{12}$$

with respect to $\{\bar{\boldsymbol{x}}_\mu\}$, $\{\bar{\boldsymbol{x}}'_\mu\}$, and $\boldsymbol{H}$ subject to the constraint $\bar{\boldsymbol{x}}'_\mu = Z[\boldsymbol{H}\bar{\boldsymbol{x}}_\mu]$, μ = 1, ..., n_1. The solution is easily obtained by modifying existing optimization techniques. We used the method of Kanatani and Ohta[3] [8].

Then, we go back to the original NM potential matches. The discrepancy of each potential match from the estimated homography is measured by

$$D_\lambda^H = \|\boldsymbol{x}'_\lambda - Z[\boldsymbol{H}\boldsymbol{x}_\lambda]\|^2, \tag{13}$$

where $\boldsymbol{x}_\lambda$ and $\boldsymbol{x}'_\lambda$ represent the two points of the λth pair, λ = 1, ..., NM. We define the confidence of global smoothness via the Gibbs distribution in the same way as the confidence of local correlations. Namely, we let

$$P_\lambda^{(2)} = e^{-tD_\lambda^H}. \tag{14}$$

The constant t is determined by solving

$$\frac{1}{Z}\sum_{\lambda=1}^{NM} D_\lambda^H e^{-tD_\lambda^H} = \bar{D}^H, \tag{15}$$

where

$$Z = \sum_{\lambda=1}^{NM} e^{-tD_\lambda^H}, \qquad \bar{D}^H = \frac{1}{L}\sum_{\lambda=1}^{L} D_\lambda^H. \tag{16}$$

The solution is easily obtained by doing Newton iterations to eq. (5) after J_λ is replaced by D_λ^H.

[3]We used the program code placed at:
http://www.ail.cs.gunma-u.ac.jp/Labo/programs-e.html

6. VOTING THE EPIPOLAR CONSTRAINT

Finally, we strictly enforce the *epipolar constraint*. For a matching pair $\{\boldsymbol{x}, \boldsymbol{x}'\}$, the *epipolar equation* is

$$(\boldsymbol{x}, \boldsymbol{F}\boldsymbol{x}') = 0. \tag{17}$$

The matrix $\boldsymbol{F}$ is called the *fundamental matrix* [6].

First, we choose candidate matches by enforcing uniqueness with respect to $P_\lambda^{(0)} P_\lambda^{(1)} P_\lambda^{(2)}$ to those pairs that satisfy

$$P_\lambda^{(0)} P_\lambda^{(1)} P_\lambda^{(2)} > e^{-3k^2/2}. \tag{18}$$

We enumerate the resulting matches by the index μ = 1, ..., n_2 in an arbitrary order. From these candidate matches, we robustly fit the epipolar equation (17) using RANSAC [4, 6]. Letting S_m = 0 and $\boldsymbol{F}_m = \boldsymbol{O}$ as initial values, we do the following computation:

1. Randomly choose eight among the n_2 pairs.
2. From them, compute the fundamental matrix $\boldsymbol{F}$.
3. For each of the n_2 pairs, compute

$$D_\mu^F = \frac{(\boldsymbol{x}_\mu, \boldsymbol{F}\boldsymbol{x}'_\mu)^2}{\|\boldsymbol{P}_{\mathbf{k}}\boldsymbol{F}^\top\boldsymbol{x}_\mu\|^2 + \|\boldsymbol{P}_{\mathbf{k}}\boldsymbol{F}\boldsymbol{x}'_\mu\|^2}, \tag{19}$$

   where $\boldsymbol{P}_{\mathbf{k}} = \mathrm{diag}(1, 1, 0)$ (the diagonal matrix with diagonal elements 1, 1, and 0 in that order).
4. Let S the sum of the confidence $P_\mu^{(0)} P_\mu^{(1)} P_\mu^{(2)}$ of those pairs that satisfy

$$D_\mu^F \leq \frac{2d^2}{f_0^2}, \tag{20}$$

   where d (pixel) is a user definable threshold[4].
5. If $S > S_m$, update $S_m \leftarrow S$ and $\boldsymbol{F}_m \leftarrow \boldsymbol{F}$.

We repeat this a sufficient number of times[5] to find the matrix $\boldsymbol{F}_m$ that gives the largest total confidence S_m.

Then, we go back to the original NM potential matches. We measure the degree of fit to the epipolar equation by D_λ^F in eq. (19) after replacing $\boldsymbol{x}_\mu$ and $\boldsymbol{x}'_\mu$, respectively, by $\boldsymbol{x}_\lambda$ and $\boldsymbol{x}'_\lambda$ that represent the λth pair, λ = 1, ..., NM. We choose from among the NM pairs those that satisfy eq. (20). The resulting pairs are thresholded by the criterion (18). Finally, we enforce uniqueness with respect to $P_\lambda^{(0)} P_\lambda^{(1)} P_\lambda^{(2)}$ to obtain the final matches.

Note that the confidence for different types of constraint can be compared or multiplied on an equal footing, because it is normalized into the interval [0,1] in such a way that the L most favorable matches have approximately the same level of confidence. This is the reason why we used the Gibbs distribution in the form of eqs. (2) and (14) and determined the attenuation constants s and t from the conditions (3) and (15).

[4]We let d = 3 in our experiment.

[5]We stopped when no update occurred for 100 consecutive iterations.

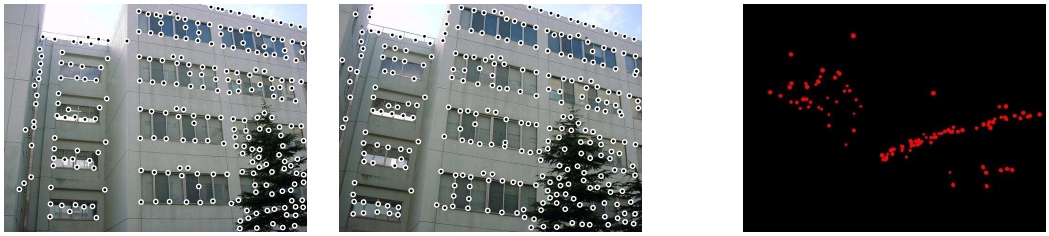

Left image. Right image. 3-D reconstruction.

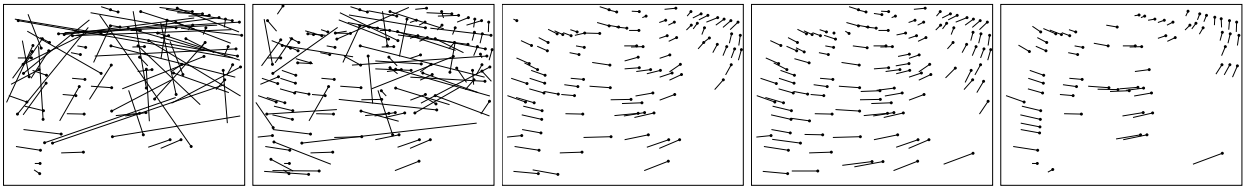

(a) (b) (c) (d) (e)

Fig. 1. Upper row: Input images and 3-D reconstruction. Bottom row: (a) Initial matches based on local correlations. (b) Matches with spatial consistency incorporated. (c) Matches with global smoothness added. (d) Final matches with the epipolar constraint imposed. (e) The method of Zhang et al. [25].

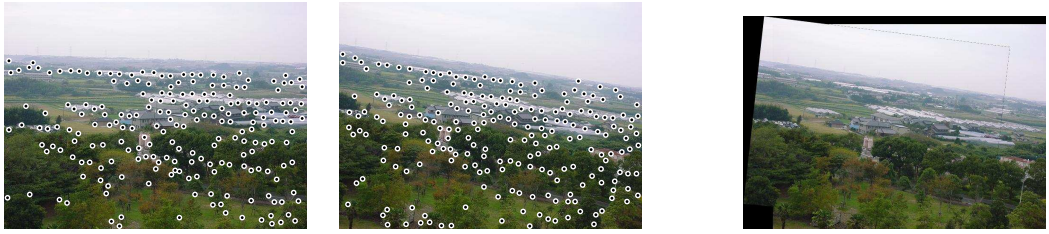

Left image. Right image. Panoramic image.

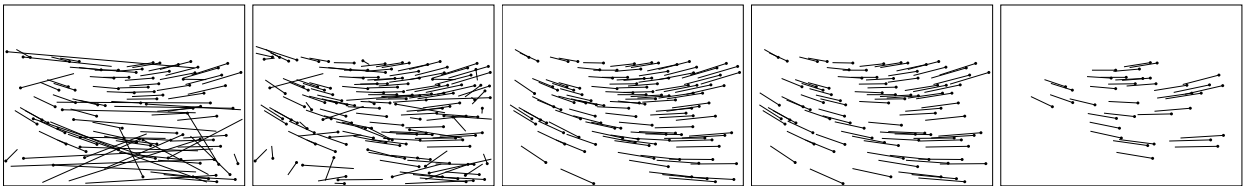

(a) (b) (c) (d) (e)

Fig. 2. Upper row: Input images and the generated panoramic image. Bottom row: (a) Initial matches based on local correlations. (b) Matches with spatial consistency incorporated. (c) Matches with global smoothness added. (d) Final matches with the epipolar constraint imposed. (e) The method of Zhang et al. [25]

7. REAL IMAGE EXAMPLES

Using the two images in the upper left of Fig. 1, we extracted 300 feature points separately using the Harris operator [5], as marked there. Fig. 1(a) is the "optical flow" of the initial candidate matches based on local correlations (we used the normalized correlation for this example). Since this scene has many periodic patterns, many mismatches exist.

Fig. 1(b) shows the matches after spatial consistency is imposed; Fig. 1(c) shows the matchers after global smoothness is added. As we can see, the accuracy increases as we impose more constraints. Doing RANSAC to the matches in Fig. 1(c), we obtained the final matches in Fig. 1(d).

For comparison, we used the method of Zhang et al.[6] [25] and obtained the flow shown in Fig. 1(e). As can be seen, our method produces denser matches than theirs. This is because matches once discarded can gain high confidence in the later stages. The upper right of Fig. 1(c) is the 3-D shape reconstructed from the computed fundamental matrix. We used the method described in [9].

Fig. 2 shows another example similarly arranged. A small camera rotation exists between the left and right images, and the scene has many similar textures. In the end, however, denser correct matches are obtained (Fig. 2(d)) than by the method of Zhang et al. [25] (Fig. 2(e)). The upper right of Fig. 2 is the panoramic image generated by the computed homography.

We then examined the effects of camera rotations. The upper row of Figs. 3 shows the left image and two right im-

[6]We used the program from placed at:
http://www-sop.inria.fr/robotvis/personnel/zzhang/softwares.html

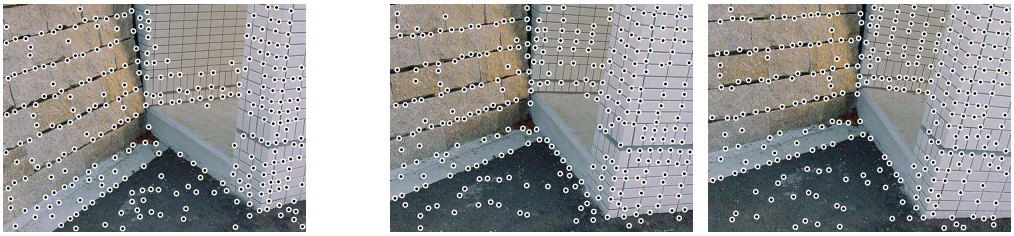

Left image. Right image 1. Right image 2.

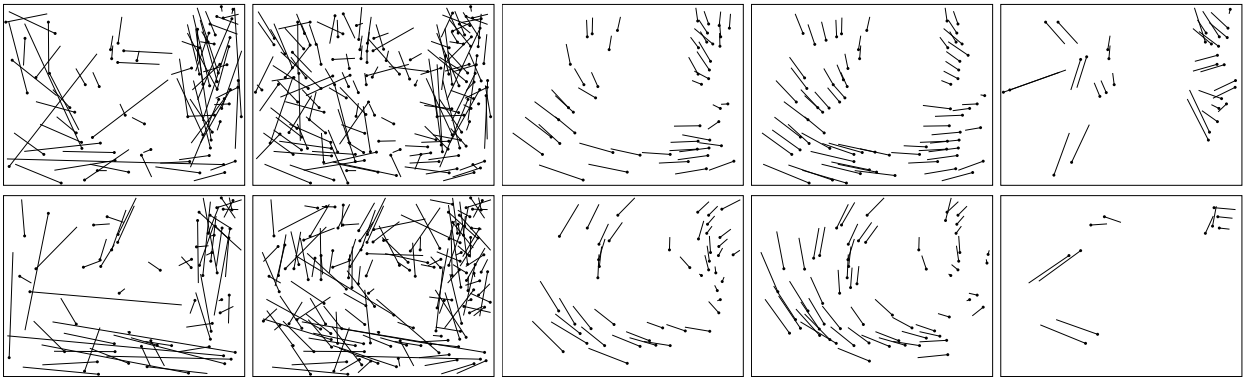

(a) (b) (c) (d) (e)

Fig. 3. Upper row: Input images. The right images 1 and 2 are rotated approximately by 5° and 10°, respectively, relative to the left image. Middle row: Results using the left image and the right image 1. Bottom row: Results using the left image and the right image 2. (a) Initial matches based on local correlations. (b) Matches with spatial consistency incorporated. (c) Matches with global smoothness added. (d) Final matches with the epipolar constraint imposed. (e) The method of Zhang et al. [25].

ages. Right images 1 and 2 are rotated approximately by 5 and 10 degrees, respectively, relative to the left image. The middle row shows the results using the left image and the right image 1; The bottom row shows the results using the left image and the right image 2. In both, (a)∼(e) correspond to (a)∼(e) in Figs. 1 and 2. As we can see, our method successfully generated sufficiently many correct matches even in the presence of camera rotations, but the method of Zhang et al. [25] failed.

We also examined the effects of zooming changes, and the results are similarly arranged in Figs. 4. This time, right images 1 and 2 are zoomed out approximately by 80% and 65%, respectively, relative to the left image. Again, our method produced a sufficient number of correct matches, while the method of Zhang et al. [25] failed.

For our examples, the total computation time (including loading image files, feature point extraction, and outputting debug information) was 23 sec on average. We used Pentium III 700MHz for the CPU with 768MB main memory and Linux for the OS.

8. CONCLUSIONS

We have presented a new method for detecting point matches between two images. Our strategy for preserving the global consistency is to impose non-local "soft" constraints on all potential matches via their "confidence values" that normalize the degree of satisfaction of different types of constraint. The confidence values are progressively updated by "mean-field approximation". Finally, the "hard" epipolar constraint is imposed by RANSAC. Using real images, we have demonstrated that our method is robust to camera rotations and zooming changes[7].

Because of our assumptions, our method works very well for smooth surfaces and distant scenes. To cope with large discontinuities is left for future research.

Acknowledgments: This work was supported in part by the Ministry of Education, Culture, Sports, Science and Technology, Japan, under the Grant for the 21st Century COE Program "Intelligent Human Sensing" and the Grant in Aid for Scientific Research C(2) (No. 15500113), the Support Center for Advanced Telecommunications Technology Research, and Kayamori Foundation of Informational Science Advancement.

9. REFERENCES

[1] P. Beardsley, P. Torr and A. Zisserman, 3D model acquisition from extended image sequences, *Proc. 4th Euro. Conf. Comput. Vision*, April 1996, Cambridge, U.K., Vol. 2, pp. 683–695.

[2] J. R. Bergen and P. Anandan, K. J. Hanna and R. Higorani, Hierarchical model-based motion estimation, *Proc. 2nd Euro. Conf. Comput. Vision*, May 1992, Santa Margerita, Italy, pp. 237–252.

[3] F. Chabat, G. Z. Yang and D. M. Hansell, A corner orientation detector, Image and Vision Computing, **17**-10 (1999), 761–769.

[4] M. A. Fischler and R. C. Bolles, Random sample consensus: A paradigm for model fitting with applications to im-

[7] The source program is available at:
http://www.img.tutkie.tut.ac.jp/programs/index-e.html

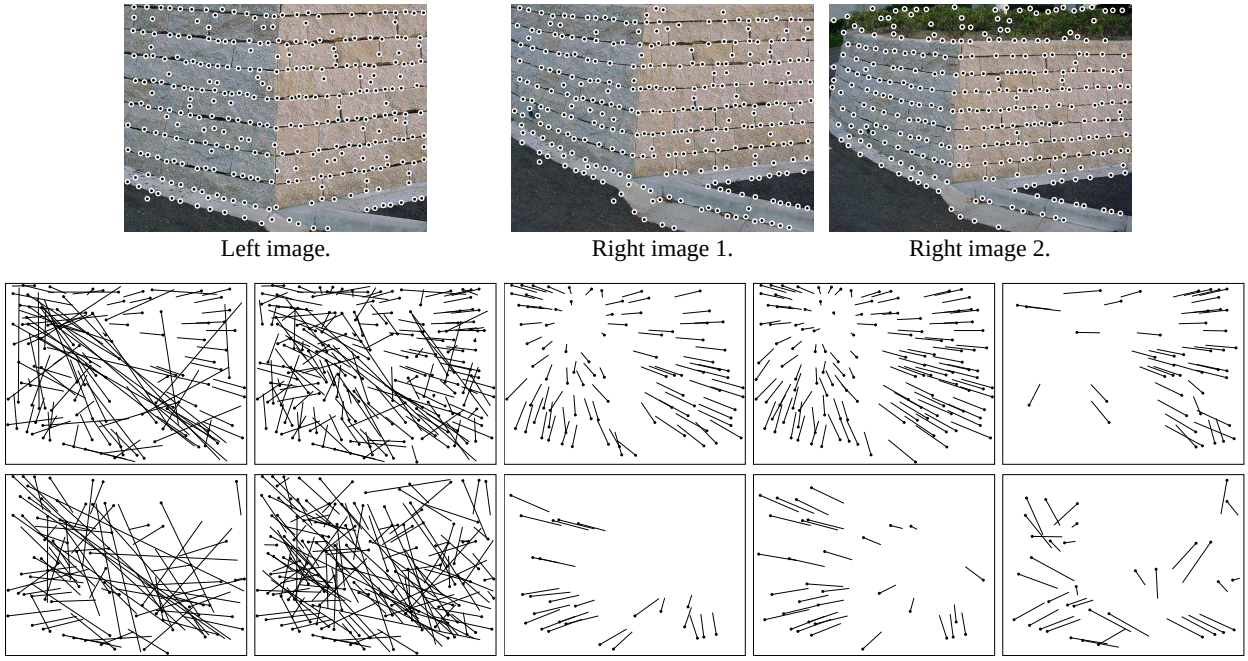

Fig. 4. Upper row: Input images. The right images 1 and 2 are zoomed out approximately by 80% and 65%, respectively, relative to the left image. Middle row: Results using the left image and the right image 1. Bottom row: Results using the left image and the right image 2. (a) Initial matches based on local correlations. (b) Matches with spatial consistency incorporated. (c) Matches with global smoothness added. (d) Final matches with the epipolar constraint imposed. (e) The method of Zhang et al. [25].

age analysis and automated cartography, *Comm. ACM*, **24**-6 (1981), pp. 381–395.

[5] C. Harris and M. Stephens, A combined corner and edge detector, *Proc. 4th Alvey Vision Conf.*, August 1988, Manchester, U.K., pp. 147–151.

[6] R. Hartley and A. Zisserman, *Multiple View Geometry in Computer Vision*, Cambridge University Press, Cambridge, U.K., 2000.

[7] K. Kanatani and Y. Kanazawa, Automatic thresholding for correspondence detection, *Int. J. Image Graphics*, **3** (2003), to appear.

[8] K. Kanatani and N. Ohta, Accuracy bounds and optimal computation of homography for image mosaicing applications, *Proc. 7th Int. Conf. Comput. Vision*, September 1999, Kerkyra, Greece, Vol. 1, pp. 73–78.

[9] K. Kanatani and N. Ohta, Comparing optimal 3-D reconstruction for finite motion and optical flow, *J. Elec. Imaging*, **12**-3 (2003), 478–488.

[10] Y. Kanazawa and K. Kanatani, Image mosaicing by stratified matching, *Workshop on Statistical Methods in Video Processing*, June 2002, Denmark, Copenhagen, pp. 31–36.

[11] M. I. A. Lourakis, S. V. Tzurbakis, A. A. Argyros and S. C. Orphanoudakis, Feature transfer and matching in disparate stereo views through the use of plane homography, *IEEE Trans. Patt. Anal. Mach. Intell.*, **25**-2 (2003), 271–276.

[12] M.-S. Lee, G. Medioni and P. Mordohai, Inference of segmented overlapping surfaces from binocular stereo, *IEEE Trans. Patt. Anal. Mach. Intell.*, **24**-6 (2002), 824–837.

[13] J. Maciel and J. Costeira, Robust point correspondence by concave minimization, *Image Vision Comput.*, **20**-9/10 (2002), 683–690.

[14] J. Maciel and J. Costeira, A global solution to sparse correspondence problems, *IEEE Trans. Patt. Anal. Mach. Intell.*, **25**-2 (2003), 187–199.

[15] C. F. Olson, Maximum-likelihood image matching, *IEEE Trans. Patt. Anal. Mach. Intell.*, **24**-6 (2002), 853–857.

[16] Pilu, A direct method for stereo correspondence based on singular value decomposition, *Proc. IEEE Conf. Comput. Vision Patt. Recog.*, Puerto Rico, June 1997, pp. 261–266.

[17] D. Reisfeld, H. Wolfson and Y. Yeshurun, Context-free attentional operators: The generalized symmetry transform, *Int. J. Comput. Vision*, **14**-2 (1995), 119–130.

[18] P. J. Rousseeuw and A. M. Leroy, *Robust Regression and Outlier Detection*, Wiley, New York, 1987.

[19] F. Schaffalitzky and A. Zisserman, Multi-view matching for unordered image sets, or "How do I organize my holiday snaps?", *Proc. 7th Euro. Conf. Comput. Vision*, May 2002, Copenhagen, Denmark, Vol 1, pp. 414–431.

[20] C. Schmid, R. Mohr and C. Bauckhage, Evaluation of interest point detections, *Int. J. Comput. Vision*, **37**-2 (2000), 151–172.

[21] S. M. Smith and J. M. Brady, SUSAN—A new approach to low level image processing, *Int. J. Comput. Vision*, **23**-1 (1997), 45–78.

[22] P. H. S. Torr and A. Zisserman, MLESAC: A new robust estimator with application to estimating image geometry, *Comput. Vision Image Understand.*, **78** (2000), 138–156.

[23] P. H. S. Torr and C. Davidson, IMPSAC: Synthesis of importance sampling and random sample consensus, *IEEE Trans. Patt. Anal. Mach. Intell.*, **25**-3 (2003), 354–364.

[24] M. A. van Wyk, T. S. Durrani and B. J. van Wyk, A RKHS interpolator-based graph matching algorithm, *IEEE Trans. Patt. Anal. Mach. Intell.*, **24**-7 (2002), 988–995.

[25] Z. Zhang, R. Deriche, O. Faugeras and Q.-T. Luong, A robust technique for matching two uncalibrated images through the recovery of the unknown epipolar geometry, *Artif. Intell.*, **78** (1995), 87–119.